Proceedings of ICRC 2001: 385 © Copernicus Gesellschaft 2001

ICRC 2001

Cosmic ray mass composition above 3×10^{17} eV measured with the Haverah Park Array

M. Ave[1], **J.A. Hinton**[2], **J. Knapp**[1], **J. Lloyd-Evans**[1], **M. Marchesini**[1], **and A. A. Watson**[1]

[1]Department of Physics and Astronomy, University of Leeds, Leeds LS2 9JT, UK
[2]Enrico Fermi Institute, University of Chicago, Chicago, IL 60637, USA

Abstract. At the Haverah Park Array a number of observables were measured that are relevant to the determination of the mass composition. In this paper we discuss measurements of the risetime of signals in large area water-Cherenkov detectors and of the lateral distribution function of the water-Cherenkov signal. The former are used to demonstrate that the CORSIKA code, with QGSJET physics, gives an adequate description of the data with a low sensitivity, in this energy range, to assumptions about primary mass. By contrast the lateral distribution is sufficiently well measured that there is mass sensitivity and we argue that in the range 0.3-0.5 EeV the data are well represented with a bi-modal composition of 30% protons and 70% iron.

1 Introduction

Here we report a mass composition analysis in the energy range 0.25-2.5 EeV that has been performed with data from the Haverah Park (HP) extensive air shower array. The HP array was a 12 km^2 air shower array consisting of water tanks that acted as Cherenkov detectors: it was operational from 1967-1987. Two parameters, $t_{1/2}$ and η, which are sensitive to the longitudinal development of showers, and hence to the mass of the initiating primary, have been studied in detail. The risetime, $t_{1/2}$, is a measure characterising the spread of the arrival times of individual particles at a given detector. It is defined as the time interval in which the integrated signal rises from 10% to 50%. Risetime data were obtained from the four 34 m^2 detectors in over 7000 events and a total of 13000 detector signals at core distances of more than 300 m (Walker and Watson, 1981). Some of these data were used to provide the first evidence that between-shower fluctuations, larger than the experimental spreads, were detectable (Watson and Wilson, 1974). The difficulty, 20 years ago, of tracking very low energy photons in space and time made it hard to interpret the observations. The second parameter, η, is a measure of the steepness of the lateral distribution function (LDF) of the Cherenkov light produced by shower particles in the water-Cherenkov detectors. It was determined with high precision using a portion of the array with a close packed detector arrangement, the so-called infilled array (Coy et al., 1997). Detailed information on the variation of η with zenith angle and energy were obtained for 1425 events in the energy range 0.25-2.5 EeV and between-shower fluctuations were also clearly established. However proper interpretation of these data, from the point of view of mass composition, was impossible as the best model calculations of the time were in gross disagreement with the data. To interpret the data detailed simulations with the CORSIKA and GEANT programs have been performed. CORSIKA (Heck et al., 1998) is a modern air shower model that simulates particle production and propagation in the atmosphere fully. It employs various models of high-energy hadronic interactions, of which the most successful is QGSJET (Kalmykov et al., 1997). The GEANT program (Brun et al., 1993) is used to account for the detector response to particles of different type, energy and impact angle.

Correspondence to: M. Ave (ave@ast.leeds.ac.uk)

2 Haverah Park Array

The Haverah Park array has been described elsewhere (Lawrence et al., 1991). The central part of the array was composed of four 34 m^2 water-Cherenkov detectors, A1-A4, spaced 500 m apart and was sensitive to showers with primary energies above $\approx 6 \times 10^{16}$ eV. Another set of three detectors (9 m^2 each) surrounding the central detector (A1) formed a 150 m array. The infilled array consisted of 28 small-area water-Cherenkov detectors located in the central region of the 500 m array with a spacing of about 150 m. The densities of Cherenkov photons per unit detector area were recorded in terms of the average signal from a vertical muon (1 vertical equivalent muon = 1 vem) per square metre. The 34 m^2 detectors provided a trigger for all detectors when the central detector (A1) and at least two out of the three other A-sites (A2, A3, A4) registered a particle density of > 0.3 vem m^{-2}. A feature of the HP array, which is particularly

important for the shower front measurements, is the area of the detectors A1-A4. These detectors allow large samples of the shower front to be taken at widely separated points, thus minimizing the chance of observing effects due only to local density fluctuations. The response of the recording system to a step function was determined by measuring the response to small showers that fell nearby and thus produced short risetimes. Cross-calibration of the detectors of the infilled array with the other detectors could have been achieved using vertical muons, as for the large-area detectors, so that they yield the same response to a purely muonic signal. However with such a cross-calibration one has to correct for the different response of the detectors to the soft component and for differences in optical and geometrical properties of the detectors and so an alternative approach was adopted. Signals from individual 2.24 m^2 and 1 m^2 detectors, next to A1, were compared with corresponding densities from the 34 m^2 detector, and an appropriate conversion factor obtained. Similar calibration procedures were used on simulations for consistency.

3 Model calculations

Using the CORSIKA code and QGSJET predictions we have generated a library of proton and iron showers with zenith angles: 0°, 15°, 26°, 40° and 45° at primary energies of 4×10^{17} eV and 6.4×10^{18} eV, and for $\theta = 26^\circ$ at energies of 0.2, 0.4, 0.8, 1.6, 3.2, 6.4, and 12.8 EeV. For each set 100 showers with the same parameters have been simulated. Additionally we have generated sets of 100 showers with oxygen and helium primaries at zenith angle 26° and energy 0.4 EeV. In total 3600 showers were produced. Statistical thinning of shower particles was applied at the level of $10^{-6} \times E_0$ with a maximum particle weight limit of $10^{-13} \times E_0$/eV. Predictions of the risetimes were deduced from the time information of each individual particle contained in the simulated shower library. The time distribution of the signals produced by electromagnetic particles for different core distances (r) was obtained for each simulated shower. The integral over the distribution was normalized to the expected signal from electromagnetic particles at the given distance for a 34 m^2 detector. The arrival time distribution of muons has been obtained for different r. The expected number of muons at a given r for a 34 m^2 detector have been computed and Poisson fluctuations added. The muons are sampled from the arrival time distribution to obtain the time distribution of the muon signal in the detector. The time distributions of the muon signal and the soft component were then added and convoluted with the known system response to an instantaneous pulse. The risetime is then inferred from the result of the convolution. This procedure was repeated 100 times for each shower to get the mean risetime as a function of r and the expected spread of the risetimes arising from Poisson fluctuations in the number of muons. To increase the statistics further each CORSIKA shower was thrown 100 times onto the array with random core positions ranging out to 300 m from the centre of the array. The risetime at each of the four 34 m^2 detectors is calculated from the parameterisations obtained above. The risetime at each detector is smeared according to an error that contains contributions from Poisson fluctuations in the number of muons and from the experimental measurement error. The core distance of each detector was fluctuated according to the error in the core positioning as described in Ave et al. (2001). To reproduce the multiplicity of measured risetimes per event in the data, we keep only the core position and the risetime of some of the detectors. We repeated this procedure for each of the 100 CORSIKA showers in a set and the mean risetime versus r (Fig. 1) is obtained. To obtain a value of η for each simulated shower we have convolved the CORSIKA output with the detector response and fitted the resulting lateral distribution function for muons and electromagnetic particles. Again, each shower was used 100 times with core positions randomly scattered over the infilled area, obtaining the densities at each detector with the parameterisations described above. The densities are modified according to Poisson fluctuations in the number of particles. We tested whether an event meets the array trigger conditions and, if so, the densities were fluctuated according to measurement errors and recorded in the same format as real data. The calibration of the infilled array is reproduced with simulations to obtain the conversion factor described in the previous section. To obtain the energy of the showers, either simulated or real, we need the $\rho(600)$-E relation and the attenuation length λ. The procedure to calculate them is described in Ave et al. (2001). The uncertainty in the core position, for the η analysis, is ≈ 5 m for all energies and primary masses tried. The energy resolution for proton primaries evolves from 15% at 0.4 EeV to 10% at 6.4 EeV, while for iron primaries it is 10% and 7%, respectively. These errors already include physical fluctuations in $\rho(600)$ and measurement errors.

4 Risetime analysis

In principle for each event, the risetime of the four 34 m^2 detectors can be recorded but, except for large and distant showers (not the subject of the present study), most often only two useful measurements are available. Therefore, the measurements were divided into θ and energy bins, and a mean risetime as function of r obtained and parameterised by a linear dependence on distance in the range $250 < r < 500$ m. Results are shown in Fig. 1 for two zenith angle ranges (21°-30° and 0°-21°) in the energy region 0.3-0.5 EeV. Results of simulations for proton and iron are also shown (see above). The flattening-off evident at the smaller core distances is a consequence of the low bandwidth of the 1970s recording system. Two cuts were applied to the data: the density in a particular detector had to be greater that 1 vem m^{-2} (to reduce sampling fluctuations), and the position of the core had to be closer than 300 m from the central triggering detector (to avoid large core errors). The dependence of the risetime on shower development arises largely because of geometry. Particle scattering, velocity differences and geomagnetic deflections are second order effects and, of course, the geometrical sensitivity is enhanced at large distances. The set of nuclear interactions that produce particles observed at an

off-axis detector may be regarded as providing a line source. There are two important properties of this line source that relate to mass composition and affect the observed risetime. These are its position in the atmosphere and its length. Previous studies of $t_{1/2}$ have revealed its dependence on θ, energy and core distance, and used deviations from mean values as measures of the variations of $X_{\rm m}$ with energy to get results on mass composition. The variations deduced (Walker and Watson, 1981) were in good accord with measurements made subsequently and directly by the Fly's Eye group (Cassiday et al., 1990). The strategy for the present analysis is different: the risetime as a function of core distance for different bins of θ and E are compared directly with predictions from Monte Carlo simulations. In the energy and distance ranges of interest here, where η has been obtained with high accuracy, the sensitivity of the risetime technique for the extraction of mass information is rather limited. The technique is, however, expected to be very effective for mass separation at greater distances and in larger showers where the mean risetime difference predicted between proton and iron showers is large and easy to measure. At small distances limitations of bandwidth mean that relatively largely samples of showers were required to establish the dependence of risetime on energy and zenith angle and to demonstrate shower-to-shower fluctuations. However this relative insensitivity to mass can be turned to advantage by using the data to test whether a shower model is able to predict average risetimes accurately over the distance range discussed here. In Fig. 1 we compare the mean risetime with distance, for two zenith angle bands, with model predictions. The data lie between the predictions for protons and iron: it is not wise to deduce any mass information from these plots because of known systematic errors in the data at the few nanosecond level. A more extensive set of comparisons will be published elsewhere. We infer from this analysis that the CORSIKA code with QGSJET physics gives a very adequate description of the mean shower risetime as a function of distance from 200-800 m. This is the first time that such agreement has been demonstrated (compare Hinton et al. (1999) in which the AIRES code with the SIBYLL particle generator was adopted). While the comparisons of Fig. 1 do not provide proof that the QGSJET model is correct they do give us reasonable confidence in using this model to attempt to interpret other data that are expected to show mass sensitivity.

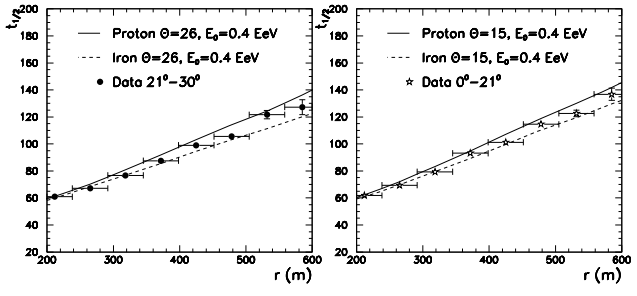

Fig. 1. Risetime versus distance to shower core in data and in simulations for proton and iron primaries

5 Lateral distribution analysis

First the shower direction was determined using the arrival time information of each individual detector. Then the particle density information was analysed to find the shower core. The lateral distribution was parameterised with respect to the known core position and the primary energy is estimated from the particle densities and the form of the lateral distribution using $\rho(600)$ in the normal way. The LDF was found experimentally to be well described by the modified power law $\rho(r) = k\ r^{-(\eta + r/4000\ \rm m)}$ in the distance range 80-800 m. Due to the small number of densities usually available without the infilled array, it was not possible to fit values of η reliably for individual showers, so no study of the fluctuations of η on a shower-by-shower basis was performed before the infilled array was set up. The algorithm used in this work to reconstruct the shower parameters is a grid search over many different core positions. For a given core position the best value of η and k are found through an analytical fit and the χ^2 function is computed. This method is different from that used originally but the results on an event-by-event basis are indistinguishable. We only used detector densities above threshold and below saturation in the range 80-800 m. Densities above saturation (9000 vem $\rm m^{-2}$) and below threshold (7 vem $\rm m^{-2}$) do not improve the fit because of the large number of well-measured densities available in each event. The selection criteria applied to the data are the following: (i) zenith angles in the range 0°-45°, (ii) in every shower the core must be located within the infilled area and (iii) showers in which the largest density is at one of the boundary detectors are excluded. After the application of these stringent criteria more than 1350 showers remain. This is the data set we use to compare with model calculations, the simulated events being analysed with the same algorithms as real data and the same cuts being applied. In the right panel of Fig. 2 the variation of η with zenith angle is shown for events with energies in the ranges 0.3-0.5 EeV and 1.0-5.0 EeV. It is evident that, if the mean mass lies between the limits of proton and iron, the lower energy data are well described by the QGSJET model. In the left panel of Fig. 2 we show the variation of η with energy. Data in three zenith angle ranges are displayed. The model calculations shown for the four mass species are for the boundary between the two most vertical zenith angle bands. In Fig. 3 the data from different zenith angles have been normalised to 26° for comparison with calculations at the same angle. The agreement between the normalised data and a smaller data set in the range $1.06 < \sec\theta < 1.16$ is good and gives confidence in the normalisation procedure. A linear fit to the normalised data is shown: the reduced χ^2 is 1.1. It should be noted that the spread from between-shower fluctuations is larger (typically 0.12) than the measurement error in η (typically 0.09). The data might be described by a single mass, independent of energy, or by a mixture of several mass components. To resolve this we use data on the spread of η. In Fig. 4a and b the experimental data in the energy band 0.2-0.6 EeV are compared with predictions for proton and iron beams. The reduced χ^2

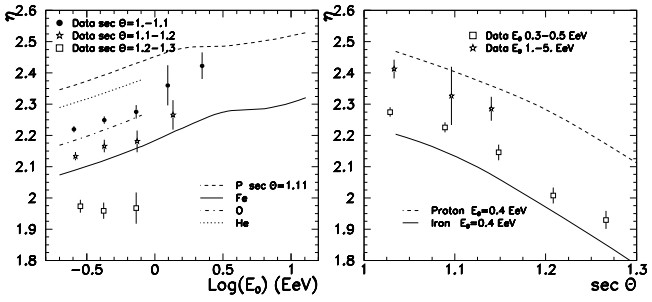

Fig. 2. Evolution of η with energy and zenith angle for data and simulation results. Left: Data at three different angle bins. The lines correspond to simulations $\sec\theta = 1.11$. Right: Data at two different energy bins. The lines indicate simulations for p and Fe at the lower energy.

for the fits are 31 and 6.4, respectively. Clearly some protons are required to fit the measurements. For helium and oxygen the corresponding numbers are 20 and 7. A fit to a dual component mixture is shown in Fig. 4c. A mixture with 29 ± 4 % of protons and a corresponding amount of iron is an excellent fit ($\chi^2/\mathrm{dof} = 1.04$): the addition of small amounts of helium and oxygen ($< 2\%$) gives $\chi^2/\mathrm{dof} = 0.8$. In Fig. 4d we show 46 events in the energy range 0.6-1.0 EeV and zenith angle range $1.04 < \sec\theta < 1.18$: a two component fit gives $30 \pm 10\%$ protons. We thus conclude that there is no evidence for any change of mass with energy in the range studied and that Fe is the dominant component. The data of Fig. 3 do not exclude the possibility of the Fe component getting larger as the energy reaches 1 EeV and then smaller beyond. However, with current understanding of model uncertainties, we consider it wise to be conservative in our claims. We note that our conclusions are not consistent with those of the HiRes-MIA group (Abu-Zayyad et al., 2001) using the same model. These authors claim that the mass composition is becoming lighter as the energy increases from 0.1 to 1.0 EeV.

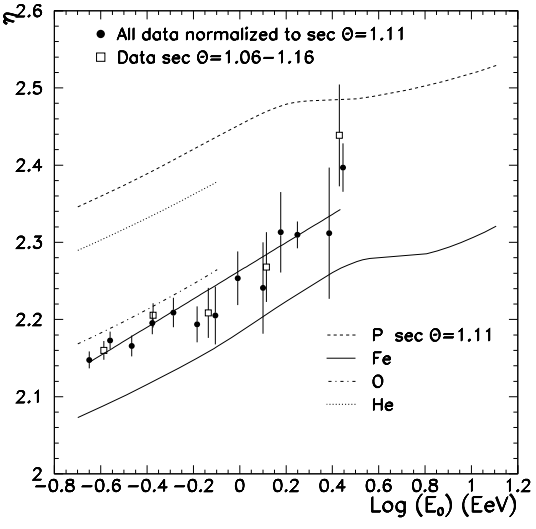

Fig. 3. Evolution of η with energy. The data are combined by normalising to 26°. The lines indicate simulations for this angle.

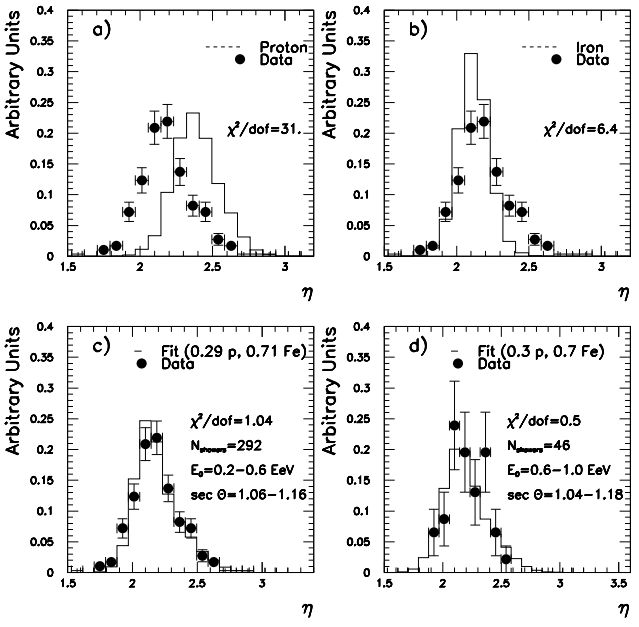

Fig. 4. η distributions for experimental data and model predictions. Panels a) and b) show that the data cannot be described by pure p of Fe composition. Panels c) and d) demonstrate for two energies that a mix of 30% p and 70% Fe yields a good fit to the data.

6 Conclusions

The mean mass composition at 0.4 EeV was obtained from HP archival data using CORSIKA and GEANT simulations. The data on lateral distributions are well fitted by a dual p/Fe composition with about 30% of the signal being protonic.

Acknowledgements. Thanks are given to members of the Haverah Park group who helped to get the data discussed here over 20 years ago. In particular the major contributions made by Dr R J O Reid are gratefully acknowledged. We also acknowledge the support of the computing centre of IN2P3 in Lyon, where the simulations were performed.

References

Abu-Zayyad T. et al., Ap. J. (to be published), astro-ph/0010652
Ave M. et al., Proc. 27^{th} Int. Cosmic Ray Conf., Hamburg (2001), HE 1.4.18
Brun R. et al., GEANT, Detector Description and Simulation Tool, CERN, Program Library CERN (1993)
Cassiday G.L. et al., Ap. J. **351** (1990) 454
Coy R.N. et al., Astrop. Phys. **6** (1997) 263
England C.D., PhD Thesis (1981), University of Leeds
Heck D. et al., FZKA 6019, Forschungszentrum Karlsruhe, 1998
Hillas A.M. et al., Proc. 12^{th} Int. Cosmic Ray Conf., Hobart **3** (1971) 1001
Hinton J. et al., Proc . 26th ICRC, Salt Lake City **3** (1999) 288
Kalmykov N. et al., Nucl. Phys. B **52B** (1997) 17
Lawrence M.A. et al., J. Phys. G **17** (1991) 733
Walker R., Watson A.A, J. Phys. G **7** (1981) 1297
Watson A.A., Wilson J.G., J. Phys. A **7** (1974) 1199